# EXHIBIT 6

Harvard Medical School

Harvard TH Chan School of Public Health

**John J. Godleski, M.D.**
*Professor of Pathology Emeritus*

Department of Environmental Health (MIPS Program)

jgodlesk@hsph.harvard.edu
Phone (617) 698-5970
Cell (617) 840-9679

June 18, 2021

**David Dearing. ESQ**
Beasley Allen Law Firm
218 Commerce Street
Montgomery, AL 36104

**Re: Carter Judkins**

Dear Mr. Dearing:

I was on the faculty of Harvard Medical School (HMS), Brigham and Women's Hospital (BWH), and Harvard School of Public Health (HSPH) from 1978-2017, retiring as Professor of Pathology in 2017. I graduated from the University of Pittsburgh School of Medicine. As a student, I did research in the Pathology Department learning electron microscopy. In my senior year, I received the top award for research done by a medical student in the United States given by the Student American Medical Association, and published several papers describing that research. I then did an internship and residency in Pathology at the Massachusetts General Hospital, a major teaching hospital of Harvard Medical School. I received further training at HSPH and the University of North Carolina. I was board certified in Anatomic Pathology in 1975. I spent 5 years on the faculty of Medical College of Pennsylvania in Philadelphia in the Department of Pathology where I was in charge of the electron microscopy facility and the autopsy service, and then was recruited to head Pulmonary Pathology at BWH in Boston, a position I held for 37 years. I published more than one hundred and seventy peer-reviewed papers related to pulmonary/environmental pathology including a number using analytical electron microscopy. Notably, I have been senior author on a number of papers using analytical electron microscopy with both X-ray analysis and electron energy loss spectroscopy. In my career, I received more than $30 million in research grants from NIH, EPA, and other funding agencies as Principal Investigator; I led the Particles Research Core in the Harvard-NIEHS Environmental Research Center and I was Associate Director of the Harvard Clean Air Research Center supported by the US EPA. In my daily activities, I was a member of the Pulmonary Pathology and Autopsy Services at Brigham and Women's Hospital. I taught Pathology residents and fellows, medical students, graduate students, and postdoctoral fellows, and I carried out research in my laboratory at HSPH. I was responsible for accurate pathological diagnoses at BWH and I oversaw a research group of as many as 15 people at HSPH. I was the pathologist providing the final opinion on difficult diagnostic cases of lung disease within our department, and I was a recognized expert whose opinion was sought by pathologists from other hospitals in the diagnosis of foreign material in tissues throughout the body using scanning electron microscopy (SEM) and energy dispersive X-ray analyses (EDS). Although now retired, I have full access to laboratory and electron microscopy facilities.

I have recently published six papers regarding talc and tissue pathology (references 1-6). The first paper used tissue digestive procedures and SEM/EDS to quantify talc in lymph nodes in comparison to the use of *in situ* SEM/EDS; the second described the migration and detection of talc in pelvic tissues from the perineum in a series of exposed patients who also had ovarian malignancy. The third concerned the use of spectroscopic magnesium and silicon weight % ratio standards to diagnose talc in human tissues, and

the expected mathematical distribution for such measurements. Three other publications also pertain to talc identification in tissue and resultant pathology (references 4-6).

I have reviewed 31 out of a possible 31 slides on Anne Judkins (SP16-53498), which represent the tissues from the patient's surgical procedure on 12/30/2016 which included hysterectomy, bilateral salpingo-oophorectomy, left and right pelvic lymph nodes excision, right para-aortic lymph nodes excision, pelvic sigmoid adhesion biopsy, and infracolic omentum biopsy. Slides on this case were received with the following sublabels: A1-4; A2-2 through A11-2; B1-2; C1-2; D1-2 through D7-2; E1-2 through E2-2; F1-2 through F3-2; and G1-2 through G6-2. Slides G1-2 through G6-2 represent the main hysterectomy specimen plus left fallopian tube and ovary, and slides A1-4 and A2-2 through A11-2 represent right ovary and fallopian tube. All slides were prepared by the Department of Pathology and Laboratory Medicine at Dartmouth-Hitchcock Medical Center (1 Medical Center Drive, Lebanon, NH 03756). The histologic slides listed above were reviewed with light microscopy, and the diagnosis of poorly differentiated serous carcinoma of the ovary was confirmed. In the surgical pathology report, the tumor was described as being in the right ovary and having a maximum dimension of 9.5 cm, with metastasis to a pelvic sigmoid adhesion. Furthermore, according to the surgical pathology report, the various lymph nodes, infracolic omentum biopsy, uterus/cervix, and left ovary and fallopian tube were all free of tumor.

The 31 histologic slides on case SP16-53498 were also reviewed using polarized light microscopy, as a means to highlight and detect birefringent foreign material in the same plane of focus with the tissues. Birefringent particle(s) were observed in 21 of the 31 slides reviewed. **Figure 1** illustrates key microscopic findings.

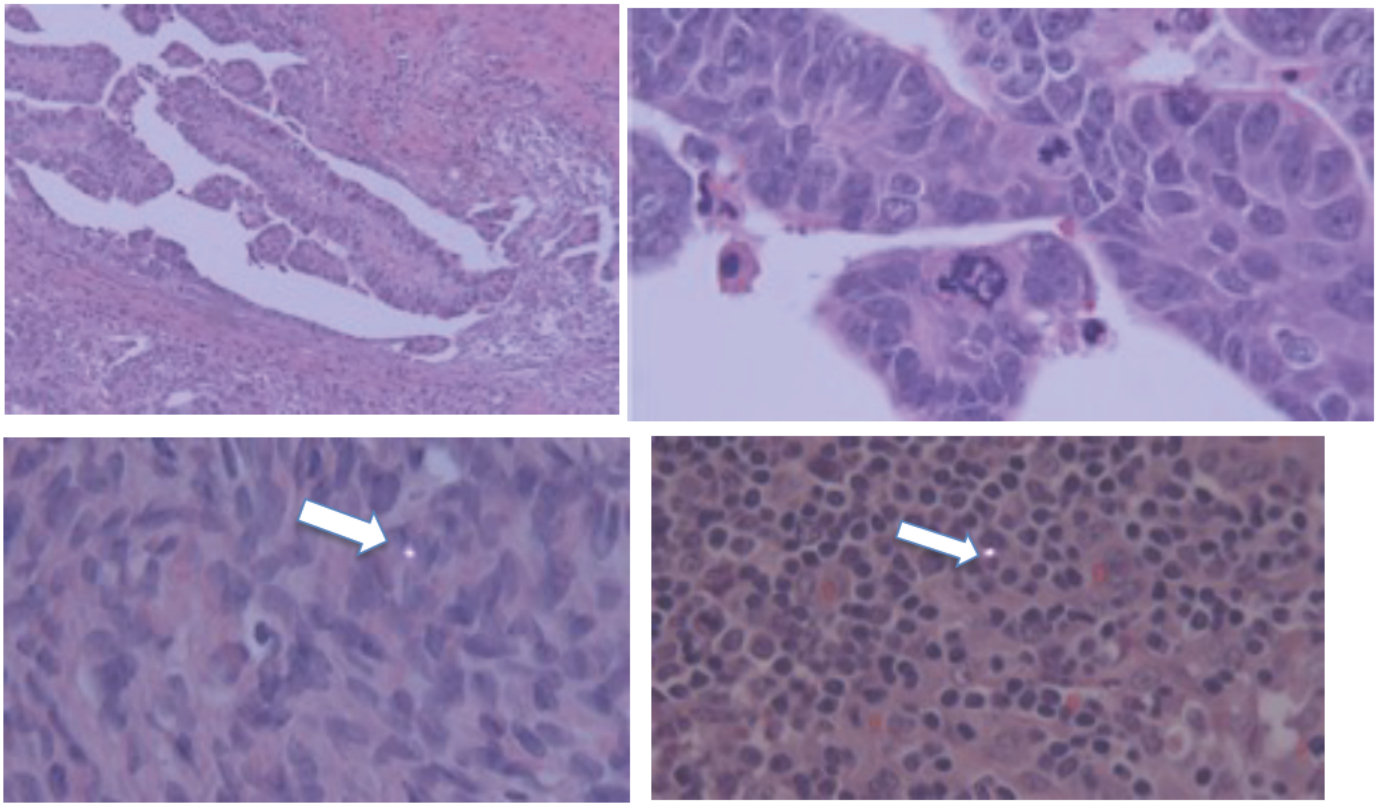

**Figure 1. Top Left.** Poorly differentiated serous carcinoma of the ovary, with associated fibrous stromal reaction. Original magnification 60x. **Top Right.** High-power view of this serous carcinoma, showing marked nuclear pleomorphism and bizarre mitotic figures. These features are characteristic of a poorly differentiated tumor. Original magnification 400x. **Bottom left.** Cellular stroma of left ovary, with a birefringent particle (see arrow) in the plane of focus with the tissues. Original magnification 400x. **Bottom right**. Right pelvic lymph node with a birefringent particle (see arrow) in the plane of focus with the tissues. Original magnification 400x. All sections stained with hematoxylin-eosin; the bottom two photos are with polarized light microscopy.

Our past experience and the medical literature on the diagnosis of talc in tissues (see references) indicate that the number of birefringent particles in histological sections is robustly correlated with the number of talc particles found by SEM/EDS, since talc is a strongly birefringent material. Also, talc is more likely to be subsequently found by SEM/EDS in tissue sections where 1) the number of birefringent particles by polarized light microscopy is greatest, and 2) the anatomic location of the tissues is most consistent with the expected migration or dissemination patterns for the talc, given its initial application/exposure site (references 1-2).

Taking these factors into consideration, we recommended that eight paraffin tissue blocks from Ms. Judkins' 12/30/2016 surgery (SP16-53498 A2, D6, D7, E1, E2, G2, G5, G6), respectively representing right fallopian tube, right pelvic and para-aortic lymph nodes, cervix, left ovary, and left fallopian tube) be obtained for further studies. All eight of these paraffin tissue blocks were received and studied as per the *in situ* scanning electron microscopy technique using variable pressure as described by Abraham and Thakral (2007, reference 7), in which the paraffin block may be studied directly in the scanning microscope chamber. The blocks were handled with our standard protocol to prevent contamination of the blocks in our laboratory. This protocol begins with the handling of the blocks using powder-free gloves on pre-cleaned surfaces. The blocks were then sectioned, removing ~50 micrometers of tissue and paraffin using a rotary microtome with a new, stainless steel blade. This sectioning was done to remove any surface contamination from previous storage and handling. After the fresh surface is exposed, the blocks were placed in a pre-cleaned covered container to prevent air particulate contamination, and then transferred to the Electron Microscopy Laboratory. There, blocks were again handled with particle-free gloves on pre-cleaned surfaces, and the blocks were washed in distilled deionized water for ≥2 minutes to remove soluble surface materials such as sodium chloride and sodium phosphate used in processing for histology. When not being examined in the SEM chamber, the blocks were always maintained in closed plastic stub container boxes to provide secure storage and to obviate lab contamination. An example of a paraffin block studied in this case is shown in Figure 2.

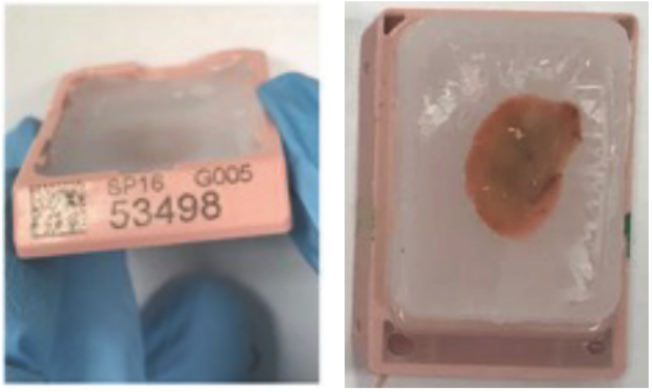


**Figure 2.** One of the blocks (G5, left ovary,) examined by SEM/EDS in this case. *Left:* The labeling (identification) for the block, which is on the side of the cassette. *Right:* Picture of the cut tissue surface of the block (examined by SEM/EDS).

Tissue surfaces were studied with a Hitachi SU6600 field emission SEM with an Oxford EDS, with Oxford instrument software being Aztec 4.1 SP1. EDS detector model was X-Max 50 SDD. The backscatter mode of the microscope was used to highlight mineral particles within the tissue resulting from atomic number contrast. Areas of tissue in the sectioned block surfaces were examined with a systematic rastering technique involving sequential fields at relatively low magnification 200-500x, then when particles were seen, higher magnification was used to show morphological characteristics and to do spectral analysis. In this study, images of backscattered or secondary electrons were acquired using 15 kV accelerating voltage, 10 mm working distance, small beam spot, aperture #1, and 60 Pa vacuum (VP-SEM mode). EDS signals were acquired in either the spot analysis or mapping mode, with dead time <20% and signal counts ~3000-5000 cps. Electron beam penetration depth under the conditions used is estimated to be 2.5 micrometers. Image files were named after the number of EDS site ID, which was consecutive from 1. Spectrum ID was also serial coded consecutively from 1. Once the images or spectra are acquired, the assigned serial ID cannot be changed or replaced.

In studying the blocks of Ms. Judkins by SEM/EDS, a total of 17 non-fibrous talc particles were found in a single ~2-micrometer plane of her tissue blocks (all listed in **Table 1** below). These particles were within

± 5% of the accepted Mg/Si atomic weight % ratio of 0.649. The majority of the talc particles (13) were found in block G5 (left ovary). A smaller, but still significant, number of talc particles were found in block G2 (cervix, 3 particles) and D6 (right pelvic lymph nodes, 1 particle). No talc was identified in the remaining five examined blocks (A2, D7, E1, E2, G6).

In the study of the blocks on this case, a total of 932 particles were found and analyzed. Tissues may have carbonaceous material detected in backscattered electron imaging mode by their surface irregularity or other characteristics. Also, in many instances iron, sodium, phosphorus, and calcium may be found in tissues, especially in patients with malignancy. These elements are all considered endogenous to the tissues in this type of study. In the tissues studied of Ms. Judkins, 483 particles had a calcium composition, either with oxygen alone, or in combination with various endogenous elements. Two hundred seventy-two (272) particles had a variety of constituents indicative of exogenous materials including 26 non-talc magnesium silicate particles sometimes with other cations, and 246 other exogenous particles which included various combinations of metals and/or silicon and/or non-metallic elements. The 17 talc particles (all in **Table 1** below) that were also found in the tissues all had magnesium and silicon in the accepted EDS spectral proportions for talc.

**Table 1: Talc block and spectrum numbers and Mg/Si atomic weight % ratios within ± 5% of 0.649**

| Block/ spectrum # | Mg/Si ratio | | Block/ spectrum # | Mg/Si ratio | | Block/ spectrum # | Mg/Si ratio |
|---|---|---|---|---|---|---|---|
| G5 197 | 0.625 | | G5 508 | 0.655 | | G5 646 | 0.660 |
| G5 318 | 0.660 | | G5 550 | 0.655 | | D6 701 | 0.660 |
| G5 425 | 0.631 | | G5 562 | 0.660 | | G2 788 | 0.655 |
| G5 426 | 0.625 | | G5 567 | 0.671 | | G2 834 | 0.631 |
| G5 430 | 0.663 | | G5 608 | 0.646 | | G2 852 | 0.655 |
| G5 435 | 0.660 | | G5 636 | 0.669 | | | |

The technique used in the study of Ms. Judkins' tissues examines an extremely small volume of tissue. Comparable studies have been done with asbestos fibers in tissue sections (reference 8), and the finding of one fiber in a tissue section comparable to the amount of tissue studied here would indicate at least 100 fibers per gram of tissue which is indicative of a substantial exposure. If similar approaches were applied to the findings of this study, indications are that very substantial amounts of talc were present in the patient's pelvic tissues. The findings of 17 talc particles spread across 3 out of 8 tissue blocks by analytical microscopy, using this approach indicates that a significant amount of talc is present within the tissues. In published studies (references 1, 2, 5, 9), significant numbers of talc particles were detected in pelvic tissues in women with ovarian cancer and a history of perineal talc use.

**Figure 3** on the following page shows the morphology of two representative talc particles detected in this case, and their EDS spectra (block G5, spectrum 608; block G2, spectrum 834). In both these instances, the atomic weight % ratio of magnesium to silicon is the ratio expected for talc (spectrum 608 = 0.646, spectrum 834 = 0.631, both within ± 5% of the accepted ratio 0.649). The magnesium, silicon, and oxygen peaks are labeled by the software of the instrument, which is periodically checked to assure that known elemental materials are properly identified.

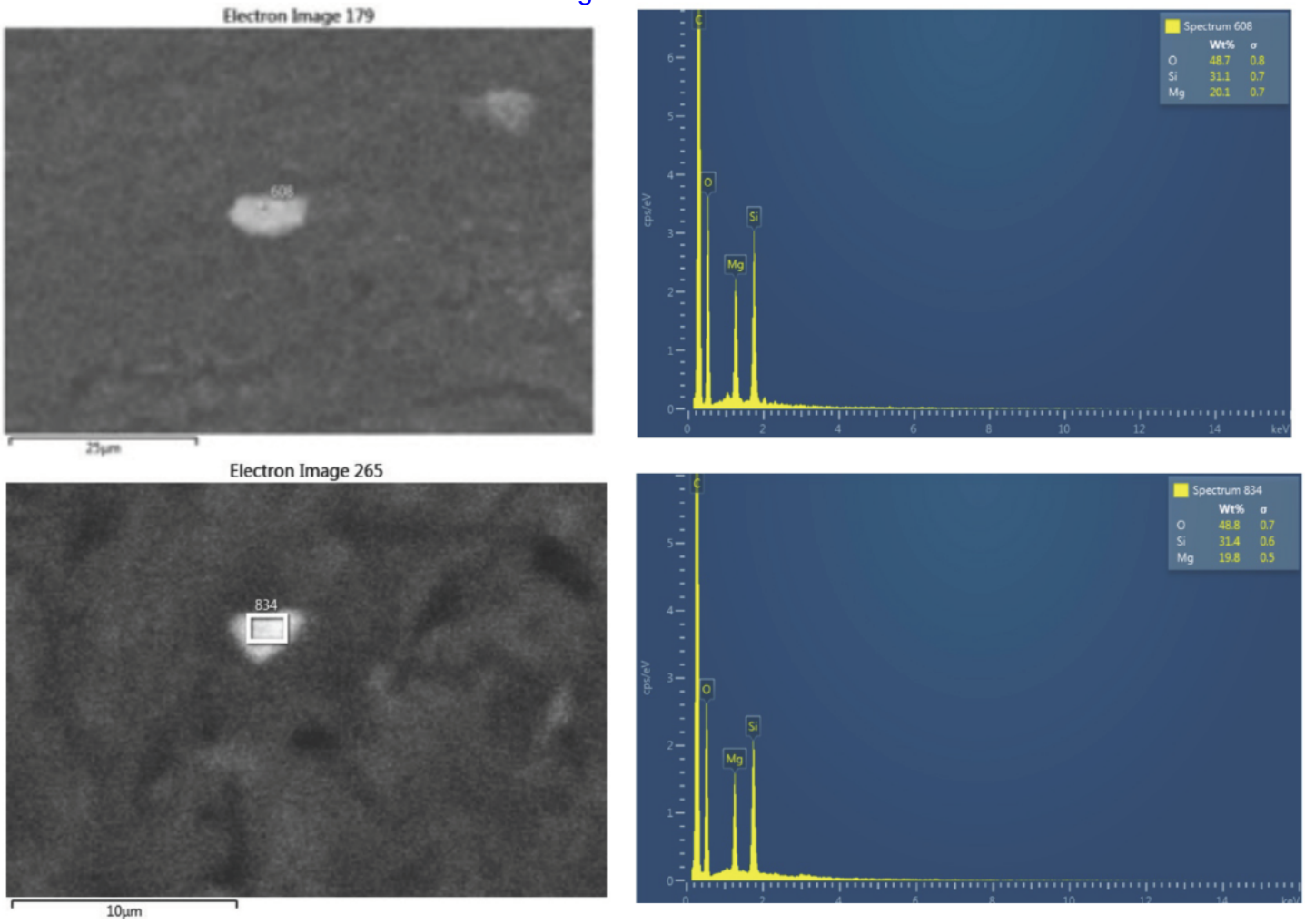


**Figure 3. Upper Left**. SEM image 179 of a particle in left ovarian tissue (block G5) in backscatter mode. This particle is within tissue and is polygonal and non-fibrous. Using the scale on the photo, the particle is ~10 microns in greatest dimension. **Upper Right**. The EDS spectrum (608) of this particle is shown with magnesium, silicon, and oxygen labeled. Magnesium and silicon have the atomic weight % ratio expected for talc, 0.646 which is within ± 5% of the accepted ratio 0.649. **Lower Left.** SEM image of a particle in cervical tissue (block G2) in backscatter mode. This particle is within tissue and is polygonal and non-fibrous. Using the scale on the photo, the particle is ~3 microns in greatest dimension. **Lower Right**. The EDS spectrum (834) of this particle is shown with magnesium, silicon, and oxygen labeled. Magnesium and silicon have the atomic weight % ratio expected for talc, 0.631 which is within ± 5% of the ratio 0.649.

Therefore, based on the findings of this case, it can be stated to a reasonable degree of medical certainty, that the talc found in this case is contributory evidence for a causal link between the presence of talc and the development of this patient's ovarian cancer. All opinions expressed in this report are to a reasonable degree of medical and scientific certainty.

Sincerely,

John J. Godleski, MD

John J. Godleski, MD
Professor Emeritus of Pathology

**References:**

1. McDonald, SA, Fan Y, Welch, WR, Cramer, DW, Stearns, RC, Sheedy, L, Katler, M, Godleski JJ. Correlative polarizing light and scanning electron microscopy for the assessment of talc in pelvic lymph nodes. Ultrastruct Pathol 43:13-27. 2019. DOI 10.1080/01913123.2019.1593271. PMID: 30898001.

2. McDonald SA, Fan Y, Welch WR, Cramer DW, Godleski JJ. Migration of talc from the perineum to multiple pelvic organ sites: five case studies with correlative light and scanning electron microscopy. Am J Clin Pathol 152: 590-607, 2019. https://doi.org/10.1093/ajcp/aqz080. PMID: 31305893 PMCID: PMC6779257.

3. McDonald SA, Fan Y, Rogers RA, Godleski JJ. Magnesium/silicon atomic weight percent ratio standards for the tissue identification of talc by scanning electron microscopy and energy dispersive X-ray analysis. Ultrastruct Pathol 43: 248-260, 2019. DOI 10.1080/01913123.2019.1692119. PMID: 31736386.

4. Campion A, Smith KJ, Fedulov AV, Gregory DZ, Fan Y, **Godleski JJ**. Identificatio**n** of Foreign Particles in Human Tissues Using Raman Microscopy Analytical Chemistry **2018** *90* (14), 8362-8369 DOI: 10.1021/acs.analchem.8b00271 PMID:29894163

5. Sato E, McDonald SA, Fan Y, Peterson S, Brain JD, Godleski JJ: Analysis of particles from hamster lungs following pulmonary talc exposures: implications for pathogenicity. Part Fibre Toxicol 2020; 17:20. https://doi.org/10.1186/s12989-020-00356-0. PMID: 32498698 PMCID: PMC7271432.

6. Johnson KE, Popratiloff A, Fan Y, McDonald S, Godleski JJ. Analytic comparison of talc in commercially available baby powder and in pelvic tissues resected from ovarian carcinoma patients. Gynecol Oncol 2020; 159: 527-533. PMID: 32977988.

7. Abraham JL, Thakral C. Automated scanning electron microscopy and X-ray microanalysis for in situ quantification of gadolinium deposits in skin. Microscopy 2007; 56: 181-187. PMID: 17951398.

8. Roggli VL, Pratt PC. Numbers of asbestos bodies on iron-stained tissue sections in relation to asbestos body counts in lung tissue digests. Hum Pathol 1983; 14: 355-361. PMID: 6299925.

9. Cramer DW, Welch WR, Berkowitz RS, Godleski JJ. Presence of talc in pelvic lymph nodes of a woman with ovarian cancer and long-term genital exposure to cosmetic talc. Obstet Gynecol 2007; 110: 498-501. PMID: